An improved U-Net architecture for simultaneous arteriole and venule segmentation in fundus image

Xiayu Xu[1,2*], Rendong Wang[1,2], Tao Tan[3,4], Feng Xu[1,2]

[1]The Key Laboratory of Biomedical Information Engineering of Ministry of Education, School of Life Science and Technology, Xi'an Jiaotong University, Xi'an 710049, P.R. China.

[2]Bioinspired Engineering and Biomechanics Center (BEBC), Xi'an Jiaotong University, Xi'an 710049, P.R. China.

[3]ScreenPoint Medical, Nijmgen, the Netherlands.

[4]Department of Biomedical Engineering, Eindhoven University of Technology, Eindhoven, the Netherlands.

*Corresponding author: xiayuxu@xjtu.edu.cn

Abstract. The segmentation and classification of retinal arterioles and venules play an important role in the diagnosis of various eye diseases and systemic diseases. The major challenges include complicated vessel structure, inhomogeneous illumination, and large background variation across subjects. In this study, we proposed an improved fully convolutional network that simultaneously segment arterioles and venules directly from the retinal image. To simultaneously segment retinal arterioles and venules, we configured the fully convolutional network to allow true color image as input and multiple labels as output. A domain-specific loss function is designed to improve the performance. The proposed method was assessed extensively on public datasets and compared with the state-of-the-art methods in literatures. The sensitivity and specificity of overall vessel segmentation on DRIVE is 0.870 and 0.980 with a misclassification rate of 23.7% and 9.8% for arteriole and venule, respectively. The proposed method outperforms the state-of-the-art methods and avoided possible error-propagation as in the segmentation-classification strategy. The proposed method holds great potential for the diagnostics and screening of various eye diseases and systemic diseases.

Keywords: Retinal vessel, segmentation, arteriole, venule, fully convolutional networks.

1. INTRODUCTION

Various eye diseases and systemic diseases manifest themselves on the fundus image as retinal vascular changes [1]. Specifically, diseases may affect the arterioles and venules differently. For example, the narrowing of retinal arterioles and widening of retinal venules independently confer long-term risk of mortality and ischemic stroke [2]. Identifying and quantifying these changes may provide useful information for the diagnosis and monitoring of these diseases. However, manual segmentation is extremely labor-intensive and clinically not feasible. Thus, it is of great importance to automatically segment and analyze arterioles and venules individually on the retinal images.

In spite of the importance, arteriole and venule classification has been one of the major challenges in retinal image analysis. The main challenges are three-fold. First, the vessel geometry (*e.g.*, diameter and tortuosity) varies a lot within one image and across different images. Second, by projecting a three-dimensional vascular structure into two-dimensional image, the vessel trees are overlapped with complicated structures. At last, the background variation between subjects is significant because of biological characteristics (*e.g.*, race and age). In literatures, the segmentation (detecting vessels) and classification (labeling vessels as arterioles/venules) have been traditionally addressed by separate modules in retinal image analysis systems [3-6]. There are several limitations in this strategy. First, the performance is sensitive to parameter choices and module selection. Second, there is error propagation in the algorithm pipeline as the classification is based on the segmentation result.

Convolutional networks have been widely applied in image labeling and segmentation in recent years. Though initially developed for image labeling, various methods have been proposed to give semantic segmentation in an image, which can be mainly classified as bounding box detection [7, 8] and semantic detection (pixel based detection) [9, 10]. In our study, the bounding box method is not feasible and semantic segmentation is desired considering the complicated vessel tree structures. In 2015, Ronneberger *et al.* proposed a U-shaped fully convolutional network (FCN) [11]. To increase the localization accuracy for fine structures, high resolution features from the contracting path are combined with the subsampled features in the expanding path. The

U-net has shown a better ability in segmenting finer structures, such as cell membrane, with very few training images. However, the original U-net has different input and output image sizes and only works on grayscale images, limiting its application to more general scenarios such as the arteriole and venule segmentation in color fundus image.

In this study, we modified and extended the architecture of the U-net. Specifically, we configure the U-net to allow true color image as input and multi-label segmentation as output. We assessed our method and compared it with literatures on public datasets.

2. Experimental Materials

The DRIVE dataset includes a set of 40 color fundus photographs obtained from a diabetic retinopathy screening program. The images were acquired using a Canon CR5 non-mydriatic 3-CCD camera with a field-of-view (FOV) of 45^{o} and a resolution of 565×584 pixels. DRIVE database is divided into two sets, each containing twenty images. The test set, which has both manual vessel segmentation and arteriole/venule labels, is included in this study. The INSPIRE dataset contains 40 optic-disc centered color fundus images with a resolution of 2392×2048 pixels [12]. Only selected vessel centerline pixels are labeled in this dataset. Arteriole centerlines, venule centerlines, and uncertain centerlines are labeled in red, blue, and white, respectively.

3. Methods

Our improved U-net model is a type of FCNs that allows end-to-end segmentations on a true color image. We employ the improved U-net to simultaneously segment both arteriole trees and venule trees in the retinal image. All three channels (i.e., red, green, and blue) are fused to allow the usage of all available information.

3.1 Preprocessing

Retinal image has a wide variation in background pigmentation, which may influence the performance of the FCN network. Image normalization by histogram matching is applied to eliminate the background differences. Histogram matching is the transformation of the histogram of an image so that it matches a specified histogram. By matching the histogram of the red, green, and blue channels individually, the algorithm can effectively match the hue of a color image to the hue of a specific image (Fig. 1).

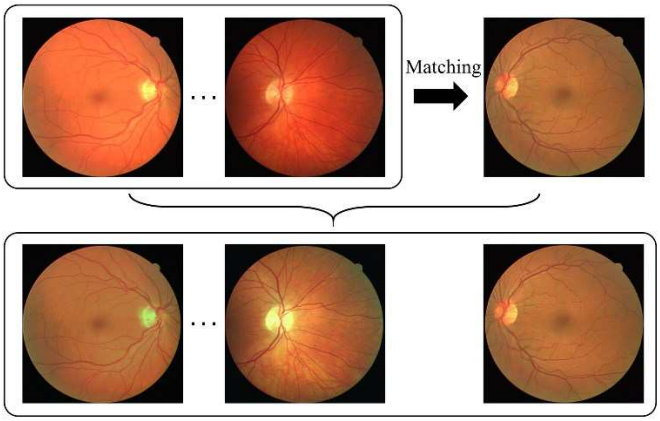

Fig. 1. Image preprocessing. First row shows the original images and second row is after histogram matching.

3.2 Training for arteriole and venule classification

The U-net can be recognized as two parts, the descending part and the ascending part. However, in the original U-net, the feature map after each convolution loses its boundary pixels, resulting in different input and output image size. We apply same padding in convolution to avoid inconsistent image sizes. The activation function is rectified linear unit (ReLU). Our network minimizes the cross entropy of a pixel-wise soft-max loss between the predicted label and ground truth label over the final feature map. The input images are resized to 576×576 pixels by linear interpolation. The detailed illustration of the architecture is given in Fig. 2. Data augmentation is implemented by applying elastic deformation [13].

Four labels are given in the original DRIVE dataset, including arterioles, venules, crossings points and unsure vessels. In this study, crossing points are considered as arterioles and unsure vessels are considered as background. The INSPIRE dataset only includes labels for selected centerline pixels and is thus excluded from training.

3.3 Testing

Before being input to the pipeline, the testing image is resized to 576×576 pixels and the mean value of each channel is subtracted from the original image. The original output is three 32-bit floating images, which contain the probabilities of each pixel belonging to each of the three categories (*i.e.*, background, arteriole, and venules).

Leave-one-out strategy is used for the DRIVE dataset. The INSPIRE dataset is tested on the network trained using DRIVE.

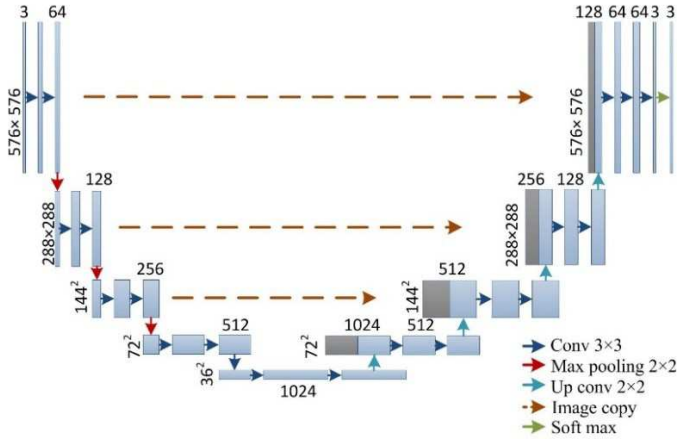

Fig. 2. Improved U-net architecture for RGB color image segmentation.

4. Results

First, we compared our vessel segmentation with the manual segmentation in a pixel-wise manner, followed by the assessment of misclassification rate of arterioles and venules. To assess the general vessel detection ability and false positive rate, we calculated the overall sensitivity (SEN) and specificity (SP), in which all arterioles and venules are regarded as vessels and otherwise considered as background.

$$SEN = \frac{TP_o}{TP_o + FN_o}, \quad SP = \frac{TN_o}{TN_o + FP_o},$$

where TP_o, TN_o, FP_o, and FN_o are the true positives, true negatives, false positives, and false negatives of all vessel segmentation, respectively. We also assessed the misclassification rate ($MISC_a$ and $MISC_v$) of arterioles and venules individually, meaning the rate of arterioles that has been misclassified as venules, and vice versa.

$$MISC_a = \frac{FP_v}{TP_a \cup FP_v}, \quad MISC_v = \frac{FP_a}{TP_v \cup FP_a},$$

where TP_a, TP_v, FP_a, and FP_v denotes the true positives of arteriole, true positives of venules, false positives of arteriole, and false positives of venule within all correctly detected blood vessels.

Visualization of original image, ground truth, and automatic segmentation results on the DRIVE dataset is given in Fig. 3. The SEN and SP of vessel segmentation is

assessed and compared with the state-of-the-art methods in Table 1. The SEN and SP of proposed method was 0.870 and 0.980. The misclassification rate was 23.7% for arteriole and 9.8% for venules. The overall classification accuracy and comparison with other methods in literatures are given in Table 2. The methods reported in literature are usually developed on known vessel segmentation and their results were also only assessed on known vessel segments or vessel centerlines. Our method, on the other hand, was assessed on all vessel pixels that are both detected by the proposed automatic method and given a ground truth label.

Visualization of the original image, ground truth, and automatic segmentation on the INSPIRE dataset is given in Fig. 4. It should be noted that the original ground truth label only contains centerline pixels for selected vessel segments, which is dilated in Fig. 4 only for the sake of better visualization. The proposed method was not trained on the INSPIRE dataset because only a small percentage of centerline pixels are provided in this dataset. For the same reason, the specificity of vessel segmentation was unable to be assessed. The overall SEN was 0.830 and the misclassification rate was 27.2% for arteriole and 13.1% for venule.

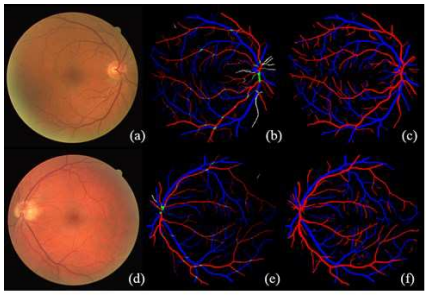

Fig. 3. Visualization of arteriole/venule segmentation on DRIVE. (a) and (d) are the original images. (b) and (e) are the ground truth labels. (c) and (f) are the results of automatic segmentation.

Table 1. Comparison of different vessel segmentation algorithms on DRIVE

Methods	SEN	SP	Time	Platform
Human	0.776	0.972	-	-
Staal *et al.[14]*	0.719	0.977	15min	1.0GHz, 1GB RAM
Ricci *et al.[15]*	0.775	0.972	-	-
Marin *et al.[16]*	0.706	0.980	~90s	2.13 GHz, 2GB RAM
Roychowdhury *[17]*	0.739	0.978	2.45s	2.6 GHz, 2GB RAM
Proposed Method	**0.870**	**0.980**	**~6s**	**GTX 1080 8GB**

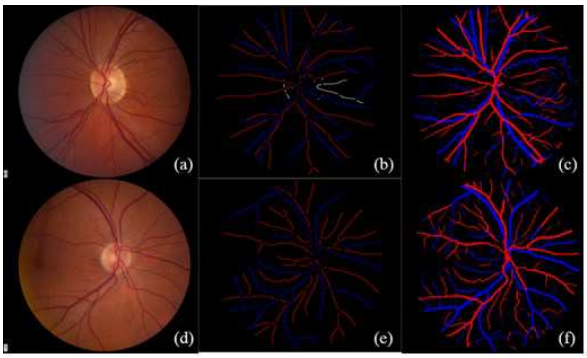

Fig. 4. Visualization typical result from the INSPIRE dataset. (a) and (d) are original color fundus images. (b) and (e) are the ground truth labels. It should be noted that the original ground truth label only contains vessel centerline pixels (single pixel width). (b) and (e) are dilated to a width of 6 pixels only for the sake of better visualization. (c) and (f) are the automatic segmentation results

Table 2. Comparison of different arteriole and venule classification algorithms in fundus image

Methods	Database	Accuracy	Description
Vazquez *et al*. [18]	VICAVR	87%	on selected major vessels
Niemeijer *et al*. [19]	DRIVE	0.88 (AUC)	on known vessel centerlines
Mirsharif *et al*. [20]	DRIVE	86%	on selected major vessels and main branches
Proposed method	**DRIVE**	**83.2%**	**on all correctly detected vessels**

5. Discussion

Applying fully convolutional networks in the segmentation of medical image is challenging because the targets are usually small or have diverse appearance or complicated structures. In this study, retinal blood vessels are fine structures with complicated tree patterns. The simultaneous segmentation of artery and vein is challenging as vessel boundary information comes from a finer scale but distinguishing artery from vein requires a coarser scale. In our approach, we take advantage of the U-net architecture, in which high resolution features from the contracting path are combined with the subsampled features in the expanding path to increase the localization accuracy for fine structures. Another advantage of our method is that it directly classifies arterioles and venules from the original image without a pre-segmentation of the blood vessels. On the other hand, algorithms

reported in the literature that show better result usually require a high-quality vessel segmentation as input.

Simultaneous arteriole and venous segmentation is the basis for other retinal image analysis towards computer-aided diagnosis, such as population-based screening of diabetic retinopathy and the measurement of arteriolar-to-venular ratio (AVR). As discussed by Estrada *et al*., though the significance of AVR has long been appreciated in the research community, the measurement of AVR has been limited to the six largest first level arterioles and venules within a concentric grid centered on the optic disc. Yet the more subtle and earlier changes in smaller arterioles and venules were not studied. The future work will be focused on a computer-aided labeling of DR signs and on the study of the association between smaller vessels and systemic diseases.

6. Conclusion

In this paper, we proposed to simultaneously segment retinal arterioles and venules using a fully convolutional network. This method allowed end-to-end multi-label segmentation of a color fundus image. We assessed and compared our method with literatures on a publicly available dataset. The result shows the proposed method outperforms the state-of-the-art methods in vessel detection and classification. This method is a potential tool for the computer-aided diagnosis of various eye diseases and systemic diseases.

REFERENCES

1. Gariano, R.F., Gardner, T.W.: Retinal angiogenesis in development and disease. Nature 438, 960-966 (2005)
2. Seidelmann, S.B., Claggett, B., Bravo, P.E., Gupta, A., Farhad, H., Klein, B.E., Klein, R., Di, C.M., Solomon, S.D.: Retinal Vessel Calibers in Predicting Long-Term Cardiovascular Outcomes: The Atherosclerosis Risk in Communities Study. Circulation 134, 1328 (2016)
3. Estrada, R., Allingham, M.J., Mettu, P.S., Cousins, S.W., Tomasi, C., Farsiu, S.: Retinal Artery-Vein Classification via Topology Estimation. Medical Imaging, IEEE Transactions on 34, 2518-2534 (2015)
4. Kondermann, C., Kondermann, D., Yan, M.: Blood vessel classification into

arteries and veins in retinal images. SPIE Medical Imaging 1-9 (2007)
5. Dashtbozorg, B., Mendonça, A.M., Campilho, A.: An Automatic Graph-Based Approach for Artery/Vein Classification in Retinal Images. Image Processing, IEEE Transactions on 23, 1073-1083 (2014)
6. Saez, M., González-Vázquez, S., González-Penedo, M., Barceló, M.A., Pena-Seijo, M., Coll de Tuero, G., Pose-Reino, A.: Development of an automated system to classify retinal vessels into arteries and veins. Computer methods and programs in biomedicine 108, 367-376 (2012)
7. Girshick, R., Donahue, J., Darrell, T., Malik, J.: Region-Based Convolutional Networks for Accurate Object Detection and Segmentation. IEEE Transactions on Pattern Analysis & Machine Intelligence 38, 142 (2016)
8. Ren, S., He, K., Girshick, R., Sun, J.: Faster R-CNN: Towards Real-Time Object Detection with Region Proposal Networks. IEEE Transactions on Pattern Analysis and Machine Intelligence 39, 1137-1149 (2017)
9. Ciresan, D., Giusti, A., Gambardella, L.M., Schmidhuber, J.: Deep neural networks segment neuronal membranes in electron microscopy images. Advances in neural information processing systems 2843-2851 (2012)
10. Shelhamer, E., Long, J., Darrell, T.: Fully convolutional networks for semantic segmentation. IEEE transactions on pattern analysis and machine intelligence 39, 640-651 (2017)
11. Ronneberger, O., Fischer, P., Brox, T.: U-Net: Convolutional Networks for Biomedical Image Segmentation. International Conference on Medical Image Computing and Computer-Assisted Intervention 234-241 (2015)
12. Niemeijer, M., Xu, X., Dumitrescu, A.V., Gupta, P., Ginneken, B.V., Folk, J.C., Abramoff, M.D.: Automated Measurement of the Arteriolar-to-Venular Width Ratio in Digital Color Fundus Photographs. IEEE Transactions on Medical Imaging 30, 1941-1950 (2011)
13. Dosovitskiy, A., Springenberg, J.T., Riedmiller, M., Brox, T.: Discriminative unsupervised feature learning with convolutional neural networks. Advances in Neural Information Processing Systems 766-774 (2014)
14. Staal, J., Abràmoff, M.D., Niemeijer, M., Viergever, M.A., Van Ginneken, B.: Ridge-based vessel segmentation in color images of the retina. Medical Imaging IEEE Transactions on 23, 501-509 (2004)
15. Ricci, E., Perfetti, R.: Retinal Blood Vessel Segmentation Using Line Operators and Support Vector Classification. IEEE Transactions on Medical Imaging 26, 1357

(2007)
16. Marin, D., Aquino, A., Gegundezarias, M.E., Bravo, J.M.: A new supervised method for blood vessel segmentation in retinal images by using gray-level and moment invariants-based features. IEEE Transactions on Medical Imaging 30, 146-158 (2011)
17. Roychowdhury, S., Koozekanani, D., Parhi, K.: Iterative Vessel Segmentation of Fundus Images. IEEE Transactions on Biomedical Engineering 62, 1738-1749 (2015)
18. Vázquez, S., Barreira, N., Penedo, M.G., Saez, M., Pose-Reino, A.: Using retinex image enhancement to improve the artery/vein classification in retinal images. Image Analysis and Recognition, pp. 50-59. Springer (2010)
19. Niemeijer, M., van Ginneken, B., Abràmoff, M.D.: Automatic classification of retinal vessels into arteries and veins. SPIE medical imaging 72601F-72601F-72608 (2009)
20. Mirsharif, G., Tajeripour, F., Sobhanmanesh, F., Pourreza, H., Banaee, T.: Developing an automatic method for separation of arteries from veins in retinal images. 1st International eConference on Computer and Knowledge Engineering (ICCKE) (2011)